PHILOSOPHICAL TRANSACTIONS OF THE ROYAL SOCIETY A

Phil. Trans. R. Soc. A (2007) **365**, 771–787
doi:10.1098/rsta.2006.1945
Published online 16 January 2007

Asymptotic scaling in turbulent pipe flow

By B. J. McKeon[1,*] and J. F. Morrison[2]

[1]*Graduate Aeronautical Laboratories, California Institute of Technology, Pasadena, CA 91125, USA*
[2]*Department of Aeronautics, Imperial College London, London SW7 2AZ, UK*

The streamwise velocity component in turbulent pipe flow is assessed to determine whether it exhibits asymptotic behaviour that is indicative of high Reynolds numbers. The asymptotic behaviour of both the mean velocity (in the form of the log law) and that of the second moment of the streamwise component of velocity in the outer and overlap regions is consistent with the development of spectral regions which indicate inertial scaling. It is shown that an 'inertial sublayer' in physical space may be considered as a spatial analogue of the inertial subrange in the velocity spectrum and such behaviour only appears for Reynolds numbers $R^+ > 5\times10^3$, approximately, much higher than was generally thought.

Keywords: asymptotic; inertial scaling; turbulent pipe flow

1. Introduction

Of late, there has been a revisiting of old questions in the scaling of wall-bounded flows. These include the scaling and self-similarity of the mean-velocity profile, Reynolds number limits for the flow to approach its infinite Reynolds number form and an assessment of the validity of the arguments for wall-bounded flows with differing geometries. The traditional belief has been that, for sufficiently high Reynolds numbers, there is a universal, self-similar form, at least at small spectral scales and sufficiently close to the wall such that the effects of large-scale geometry are not felt, yet sufficiently remote from it so that the turbulence can approach approximate local isotropy. We seek here to explore the approach of the turbulent flow to an asymptotic scaling, narrowing the focus to fully developed pipe flow and building on results of Zagarola & Smits (1998) and McKeon *et al.* (2004) that addressed the question of complete similarity of the mean velocity profile, and of Morrison *et al.* (2004) which examined the scaling of the higher moments. In particular, we address the links between physical and spectral scaling regions which may be deemed inertial in the sense that energy transfer is the dominant mechanism of the spectral energy budget. By 'transport' we mean a spatial flux, while the term 'transfer' is used to mean a spectral flux. By implication, there is significant separation between the scales at which turbulent energy production and dissipation occur, and thus the Reynolds

* Author for correspondence (mckeon@caltech.edu).

One contribution of 14 to a Theme Issue 'Scaling and structure in high Reynolds number wall-bounded flows'.

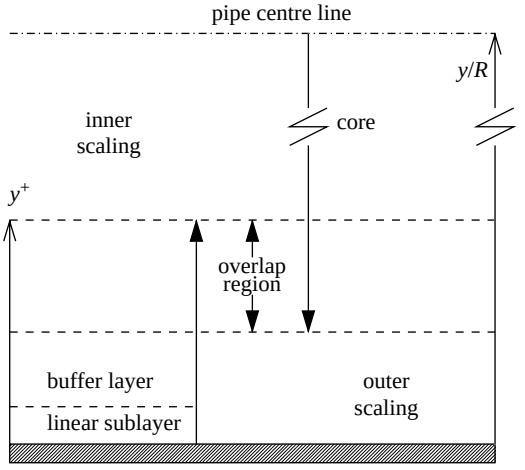

Figure 1. Schematic of mean velocity scaling in fully developed pipe flow.

number must be 'high'. We are concerned here with the Reynolds number regime in which there is an approach to the scaling of turbulence occurring at infinite Reynolds number rather than expressions that take into account low Reynolds number effects, such as a so-called 'generalized log law' or a Reynolds number-dependent power law. While the approach can be slow, conditions under which the turbulence cannot be said to approach its asymptotic form may be identified.

Consider first the requirements for high Reynolds number scaling of the mean velocity, U, with wall-normal distance, y. The classical form of a logarithmic law may be derived using an overlap argument (Millikan 1938) for a region where there is sufficient separation of inner and outer scales, namely $y^+ \gg 1$ and $y/R \ll 1$

$$U^+ = \frac{1}{\kappa} \ln y^+ + B. \tag{1.1}$$

κ and B are known as the von Kármán and additive constants, respectively, and have values in the region of $\kappa = 0.4$ and $B = 5.0$. Here, R is the outer length-scale (the pipe radius) and $^+$ denotes non-dimensionalization by the wall variables, the friction velocity $u_\tau = \sqrt{\tau_w/\rho}$ and viscous length-scale ν/u_τ. τ_w is the time-averaged wall shear stress, ρ is the fluid density and ν is the kinematic viscosity. This analysis assumes that u_τ is the appropriate scaling velocity for both inner and outer regions, where if the Reynolds number is high enough, the influence of viscosity in the outer region appears only through the scaling of u_τ. A schematic of the classical, high Reynolds number wall-normal variation of the mean velocity is given in figure 1.

Logarithmic scaling of the mean velocity may also be deduced for a 'constant-stress' layer ($-\overline{uv} = u_\tau^2$, where $-\rho\overline{uv}$ is the Reynolds shear stress) by use of the 'local-equilibrium' approximation, namely

$$\epsilon = \Pi = -\overline{uv}^+ \frac{u_\tau^3}{\kappa y} = -\overline{uv} \frac{\partial U}{\partial y}, \tag{1.2}$$

in which the rate of production, Π, is balanced by the energy dissipation rate, ϵ. The approximation that energy is dissipated close to where it is produced in this region becomes more accurate as the Reynolds number increases so that the *net* spatial transport becomes negligible and, because transport constitutes a source

or sink at each wavenumber, spectral transfer dominates the spectrum. It is for these reasons that the region of self-similar logarithmic scaling in the mean velocity is commonly referred to as the 'inertial sublayer'.

With either inner or outer scaling, the log law requires that, for $R^+ \to \infty$, the mean velocity obeys, simultaneously, the law of the wall $U^+ = f(y^+, R^+) \to f(y^+)$ and the velocity defect law, $U^+_{\mathrm{cl}} - U^+ = g(y/R, R^+) \to g(y/R)$ independent of Reynolds number. Here cl denotes centreline conditions. However, the requirement for local equilibrium presents a rather stronger condition than an overlap argument and the implications of this are analysed here.

Marati *et al.* (2004) have explored spatial and spectral energy fluxes in Poiseuille flow using a low Reynolds number direct numerical simulation. They suggested that, as the Reynolds number increases, the role of inhomogeneity is expected to decrease so that the logarithmic region can be described as a local region of approximately homogeneous turbulence under weak local shear with a superimposed, constant, spatial flux of energy passing across it from the wall to the outer flow. Energy produced at scales of the order of the shear scale $S^* = \sqrt{\epsilon/S^3}$ (which can be considered as the ratio of the characteristic mean strain rate to the inertial transfer time, where $S = \mathrm{d}U/\mathrm{d}y$ is the local wall-normal velocity gradient), is dissipated close to the Kolmogorov microscale, $\eta = (\nu^3/\epsilon)^{1/4}$.

In the limit of high Reynolds number, the behaviour of the energy dissipation rate is encapsulated in the so-called 'zeroth law' of turbulence. Taylor (1935) proposed that, above a minimum Reynolds number based on the Taylor scale $\lambda_{\mathrm{T}} = \overline{u^2}/\overline{(\partial u/\partial x)^2}$, $C_\epsilon = \epsilon l/u^3 \to$ constant; i.e. the non-dimensional dissipation rate tends to a finite, positive value. The typical energy-containing length and velocity scales are l and u, respectively. A large body of experimental data, mostly from grid turbulence (e.g. Sreenivasan 1998), identifies Taylor's critical Reynolds number between 50 and 200, most generally $R_{\lambda \mathrm{T}} \approx 100$. However, the constant, C_ϵ, does not appear to be universal and is flow-dependent. In the overlap region of a wall-bounded flow, approximate local equilibrium may be said to have been established when $C_\epsilon \simeq \epsilon y/u_\tau^3 \approx 1/\kappa$. The lower limit for the zeroth law may be assessed in the local-equilibrium region by expressing the Taylor microscale Reynolds number as

$$R_{\lambda \mathrm{T}} = \frac{\lambda_{\mathrm{T}} \sqrt{\overline{u^2}}}{\nu} = \frac{\overline{u^2}^+ \sqrt{15 \kappa y^+}}{-\overline{uv}^+}. \tag{1.3}$$

Inertial scaling in the velocity spectrum of turbulence was proposed by Kolmogorov (1941; henceforth 'K41') as part of a universal spectral scaling for wavenumbers, k, where the turbulent fluctuations are locally isotropic and therefore independent of the large-scale features of the flow. Then the Kolmogorov length-scale is the only relevant scale and the energy spectrum can be expressed in a self-similar form. With the assumption of local isotropy, the expected scaling of the u-component spectrum, $\phi_{11}(k_1)$, can be written

$$\phi_{11}(k_1) = \epsilon^{2/3} k_1^{-5/3} f(k_1 \eta). \tag{1.4}$$

In a wavenumber range that is independent of viscosity, where the forcing and dissipation scales are sufficiently well separated so that only the inertial terms dominate the energy budget, Kolmogorov proposed that $f(k_1\eta) \to C_{\mathrm{K}}$ for $k_1 \eta \ll 1$, where C_{K} is a constant—the so-called $k^{-5/3}$ scaling. This universal scaling has been most straightforwardly sought in homogeneous, isotropic turbulence.

While there is little data to contradict Kolmogorov's ideas in asymptotic form, some questions remain open, including the increasing admittance of the effects of boundary conditions or 'intermittence' as described in Kolmogorov (1962) and the necessary Reynolds number to achieve a constant value of C_K and exponent of $-5/3$ (e.g. Mydlarski & Warhaft 1996).

In wall-bounded flows, the simultaneous effects of both shear and blocking of a non-porous boundary must also be considered. In inhomogeneous shear flows, Ferchichi & Tavoularis (2000) have documented the persistence of anisotropy in the smallest scales at the highest Reynolds number of their experiment ($Re_{\lambda T} \approx 660$), but suggested that the anisotropy decayed with increasing Reynolds number, consistent with K41. In the presence of a wall, the classical picture of energy transfer requires further modification to take account of the spatial fluxes that arise due to the wall-normal inhomogeneity imposed by the no-slip boundary condition. Moreover, anisotropy, usually explained as the consequence of the different ways in which the impermeability and viscous constraints affect the near-wall motion, leads to inter-component transfer. While this effect tends to be prevalent at low wavenumbers, there is likely to be a residual influence in the small scales as well.

In the overlap region, however, the 'local-equilibrium' approximation suggests that energy is dissipated close to where it is produced, and owing to the limited spatial transport, it is a sensible location to assess $k^{-5/3}$ or inertial scaling. An approach to local isotropy in wall-bounded flows can be questioned on fundamental grounds due to the effect of mean strain on the anisotropy of the dissipation tensor, e.g. Durbin & Speziale (1991), and the increasing influence of boundary conditions with Reynolds number through spatial intermittency as detailed in K62. However, experimental observations of $k^{-5/3}$ scaling in wall-bounded flows are useful, especially in the absence of firm conclusions concerning local isotropy. It is clear, however, that $k^{-5/3}$ scaling is not necessarily an indication of local isotropy. The insensitivity of $k_1^{-5/3}$ scaling as an indicator of local isotropy has been noted by Lawn (1971), Mestayer (1982) and, in comparison with the second-order longitudinal structure function, Frisch (1995), among others.

Bradshaw (1967) observed $k_1^{-5/3}$ scaling (streamwise wavenumber) in a boundary layer at moderately high Reynolds number and proposed a 'first-order' inertial subrange, for which a sufficient condition is that production and dissipation are a small fraction of the inertial transfer only: local isotropy is not a necessary requirement. Saddoughi & Veeravalli (1994) investigated Kolmogorov scaling in a very high Reynolds number boundary layer, $Re_\theta = 3.7 \times 10^5$ (θ is the momentum thickness) and proposed conditions for various levels of approximation to local isotropy.

The presence of inertial scaling in the spectrum can be attributed to a suitable separation of energy-containing and dissipative scales, or local turbulence Reynolds number. As developed by George & Castillo (1997) and Wosnik *et al.* (2000) in their scaling theories for zero-pressure-gradient boundary layer and internal flows, respectively, this also has strong implications for the scaling of the mean velocity. Even at high Reynolds number, there remains a region near the wall in which the shear stress is approximately constant but there is insufficient scale separation for inertial scaling. Wosnik *et al.* (2000) suggest that inertial scaling is not observed until at least $R^+ > 3 \times 10^3$ in internal flows. Note that this

Table 1. Resolution of hot-wire measurements.

Re_D	R^+	l/d	$k_1\eta_{\min}$	$TU_{\rm cl}/R$
55×10^3	1.50×10^3	200	1.60	2.20×10^5
75×10^3	1.82×10^3	200	1.10	3.26×10^4
150×10^3	3.35×10^3	200	0.86	3.20×10^4
410×10^3	8.56×10^3	100	0.85	2.13×10^4
1×10^6	19.7×10^3	100	0.37	8.45×10^3

'mesolayer' is different in origin to the proposal by Long & Chen (1981) of a region close to the peak in Reynolds stress in which the influence of both viscosity and the outer length-scale remain important.

There has been more investigation of the spectral form of the larger, energy-bearing turbulent scales (e.g. Morrison *et al.* 2004). In the overlap region, both inner- and outer-scaled spectral regions contribute to the energy, such that there are regions of spectral collapse with Reynolds number and wall-normal distance under either y scaling or R scaling (but there is no evidence of simultaneous collapse in pipe flow). Turbulence intensities scaled on outer variables first display similarity for sufficiently high Reynolds numbers, $R^+ > 1.8\times10^3$.

The data analysed here were taken in the Princeton/ONR 'Superpipe', a compressed air facility capable of a wide Reynolds number range, $31\times10^3 \le Re_D = \bar{U}D/\nu \le 35\times10^6$, which approaches the Reynolds numbers obtained in industrial piping such as a transcontinental natural gas pipelines. D is the pipe diameter and $\bar{U}$ is the volume-averaged velocity. Zagarola & Smits (1998) and McKeon *et al.* (2005) reported Pitot tube measurements of the mean velocity, and Morrison *et al.* (2004) detail single normal hot-wire measurements of the fluctuating streamwise velocity. Details of the facility can be found in Zagarola (1996) and Zagarola & Smits (1998; henceforth 'ZS').

We begin by reviewing, with some extension, high Reynolds number results for the streamwise velocity, before presenting observations on the spectral scaling of the small streamwise scales and placing them in the context of the relationship between inertial scaling in physical and spectral space. The focus is limited to the overlap region because it is a well-conditioned area for study: the local-equilibrium approximation applies and is used to provide estimates of ϵ. Isotropic estimates, $\epsilon = 15\nu\overline{(\partial u/\partial x)^2}$, are avoided owing to the limitations set by probe resolution. The momentum equation yields an accurate estimate of the shear stress, $-\overline{uv}^+ = 1 - y/R - 1/(\kappa y^+)$, $\overline{u^2}$ is obtained from Morrison *et al.* (2004) and $\kappa \approx 0.4$.

Morrison *et al.* (2004) provide details concerning the normal hot-wire measurements, obtained for $55\times10^3 \le Re_D \le 5.7\times10^6$. Owing to the large Reynolds numbers, it is important that the spatial resolution of the hot wires (0.5 mm in length) is addressed. While the spatial resolution is often given in terms of the ratio of the wire length to the viscous length-scale, l^+, it is clear that a more appropriate measure is $k_1\eta|_{\max} = 2\pi\eta/l$, where, for example, by use of the local-equilibrium approximation, $\eta^+ = (\kappa y^+)^{1/4}$. Thus, the constraint on spatial resolution is the most stringent close to the wall, where η is smaller. The value of y^+ for the measurement point closest to the wall increases as the Reynolds number increases such that the lower limit of the log law cannot be explored in all experiments. Details of probe resolution are given in table 1, and in all cases $k_1\eta = 2\pi\eta/l \ge 0.37$, and mostly ≥ 0.85.

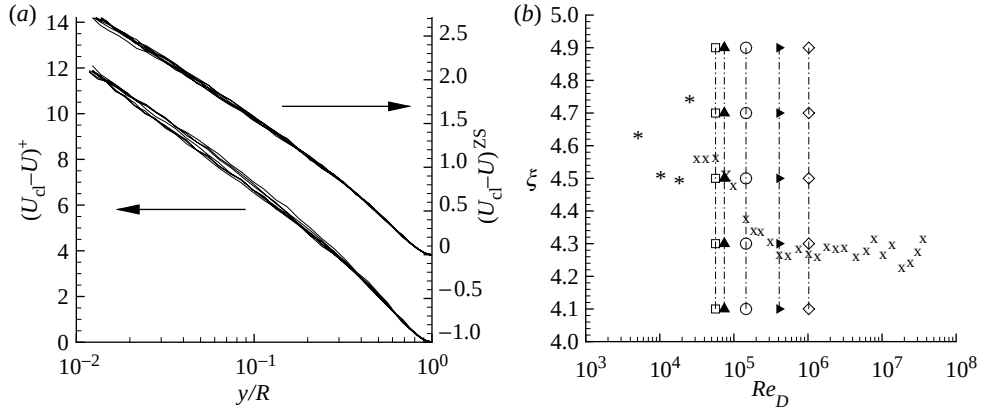

Figure 2. (*a*) Variation of the outer scaled mean velocity defect using classical (left axis) and ZS (right axis) velocities and (*b*) variation of $\xi = (U_{cl} - \bar{U})/u_\tau$ with Re_D. Cross, present data; asterisk, from den Toonder & Nieuwstadt (1997). Large symbols used to denote specific Reynolds numbers: open square, 55×10^3; filled triangle, 75×10^3; open circle, 150×10^3; right side filled triangle, 410×10^3; open diamond, 1×10^6.

Thus it is expected that, even at the highest Reynolds number, effects of spatial resolution are confined to the dissipation range only. The sampling frequency is adjusted so that it is better than the spatial resolution divided by the largest convection velocity—taken to be the pipe centre line mean velocity.

2. The mean velocity profile

Zagarola & Smits (1998) presented the first investigation of the mean velocity scaling in the Superpipe for Reynolds numbers in the range $31\times10^3 \leq Re_D \leq 35\times10^6$. Subsequently, McKeon *et al.* (2004, 2005) used high Reynolds number probe corrections to reduce both Zagarola's data and a second set of data obtained using a smaller Pitot probe. A picture of distinct changes in the mean velocity profile with increasing Reynolds number emerges from these data.

While other studies, e.g. den Toonder & Nieuwstadt (1997), have also demonstrated that the law of the wall is established at relatively low Reynolds numbers, the wide Reynolds number range in the Superpipe data revealed that outer similarity of the mean velocity (using u_τ as the outer velocity scale) is not observed until surprisingly high Reynolds numbers. Figure 2*a* demonstrates that u_τ collapses the mean velocities in the pipe core with only reasonable success, and it is the lower Reynolds number data which fail to collapse, suggesting that the flow is still developing and/or inappropriate velocity scale selection. The outer velocity scale proposed by ZS, $U_{cl} - \bar{U}$, is rather more successful in collapsing the velocity defect in the outer region, also shown in figure 2*a*. As such, this velocity scale may be taken as a measure of large eddies detached from the wall, so more appropriate to a wake-like outer flow. For high Reynolds numbers, of course, the ratio of the ZS scale to the friction velocity, ξ, reaches a constant value, as demonstrated in figure 2*b*. ξ must be a constant for complete similarity of the mean velocity profile (by consideration of the integration of a logarithmic profile,

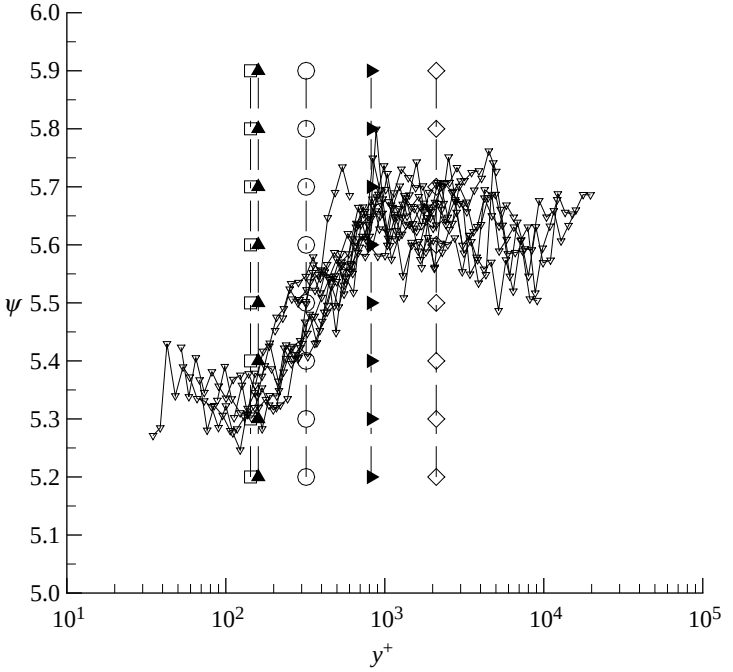

Figure 3. Mean velocity deviation, ψ, from the log law with y^+ for $y/R<0.12$.

Yaglom 1979), so that either velocity can be used for scaling purposes. It can be seen that $\xi=4.28$ only for $Re_D \geq 310\times10^3$ ($R^+>5\times10^3$). This, therefore, represents a lower limit of Reynolds number for which a Reynolds number-independent logarithmic scaling is possible in the mean velocity. This trend is also present in the classical data of Nikuradse (1932), not shown.

The validity of the log law was determined by McKeon *et al.* (2004) from consideration of the inner-scaled deviation function, ψ, where

$$\psi = U^+_{\mathrm{meas}} - \left(\frac{1}{\kappa}\ln y^+\right), \tag{2.1}$$

with $\kappa=0.42$, shown in figure 3. $\psi=$constant (and a log law with the given value of κ) is a good fit to the data for which $B=5.60\pm0.05$ for $y^+>600$, approximately, and $y/R<0.12$, i.e. when $R^+>5000$. For $50<y^+<300$, the data are well described by a power law, and this expresses the direct influence of viscosity out to $y^+\approx0.12R^+$ when $R^+<5000$.

The von Kármán constant was determined from the scaling of the friction factor with Reynolds number in McKeon *et al.* (2005), an integral constraint which removes the ambiguities associated with differentiation of mean velocity profiles. It was found that there was no Reynolds number dependence of the friction factor scaling for $R^+>5000$, within the experimental error of 1.1%, in excellent agreement with the indication from the variation of ψ that a log law would not be observed below a minimum Kármán number of $R^+=600/0.12=5\times10^3$ and the Reynolds number required for a constant value of ξ. The y^+ locations of the outer edge of the overlap layer (at which $y/R\approx0.1$) for the Reynolds numbers indicated by the symbols in the legend of figure 2 are also

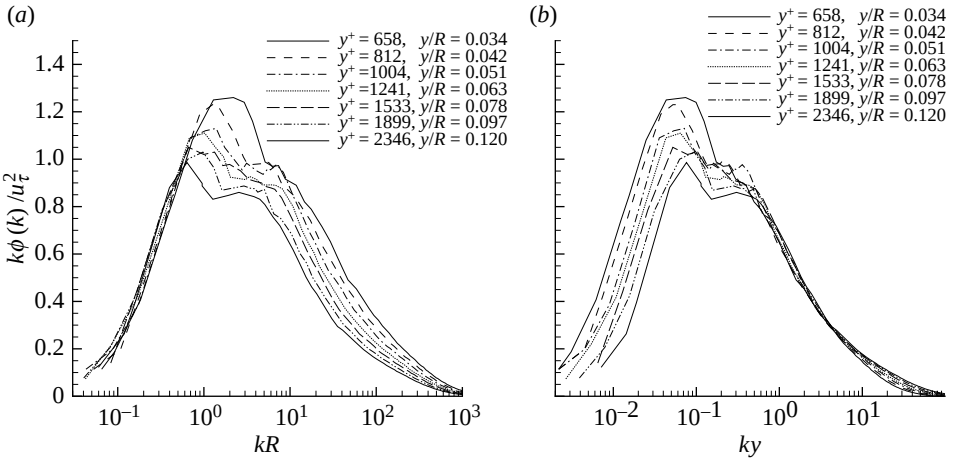

Figure 4. Compensated spectra at $Re_D = 1\times10^6$ in (*a*) outer and (*b*) inner scaling.

shown in figure 3. It can be seen that the distinct changes in the shape of ψ occur at the same conditions as those in ξ, indicating the consistent nature of changes in the mean velocity profile with increasing Reynolds number.

3. Spectral scaling of the streamwise velocity

The scaling of the streamwise velocity spectrum in the low- and mid-wavenumber ranges was explored in Morrison *et al.* (2004). Figure 4*a*,*b* shows pre-multiplied spectra with outer and inner scaling, respectively, for increasing wall-normal distance at $Re_D = 1.0\times10^6$ ($R^+ = 19.7\times10^3$). There are clearly extensive regions of collapse in outer (R) and inner (y) scaling, but not in the same ranges of wavenumber.

Inner scaling fails when the wavenumber becomes so small that scales on the order of the pipe radius become important. Note that the influence of these 'very large-scale motions' (VLSMs) increases with Reynolds number (Kim & Adrian 1999). Spectra at a constant wall-normal location close to the outer edge of the overlap layer, $y/R = 0.1$, in figure 5*a* confirm that these large motions are significantly less pronounced at $Re_D = 55\times10^3$ than at $Re_D = 1.0\times10^6$.

With this pre-multiplication, self-similar k^{-1} scaling would appear as collapse to a (universal) constant for the same wavenumber range in both the plots. It can be seen that the large energy content of the VLSMs dominates the spectrum in the wavenumber regime $R^{-1} \ll k_1 \ll y^{-1}$, such that the spectral energy decreases as y increases. There is no evidence for a region where both inner and outer scaling are valid. Note, however, that Nickels *et al.* (2005) have observed a limited region of k^{-1} scaling (one-third of a decade) closer to the wall in a similar Reynolds number boundary layer.

Figure 5*b*, from Morrison *et al.* (2004), shows the variation with y of the energy in the streamwise velocity component, plotted with outer scaling in the form $\overline{u^2}^{ZS}$ for a wide range of Reynolds numbers. For $y/R > 0.4$, the data collapse in two distinct groups, one for $Re_D < 75\times10^3$ and another for $Re_D < 230\times10^3$ with the data at 75×10^3 lying between the two. In each branch, the region of

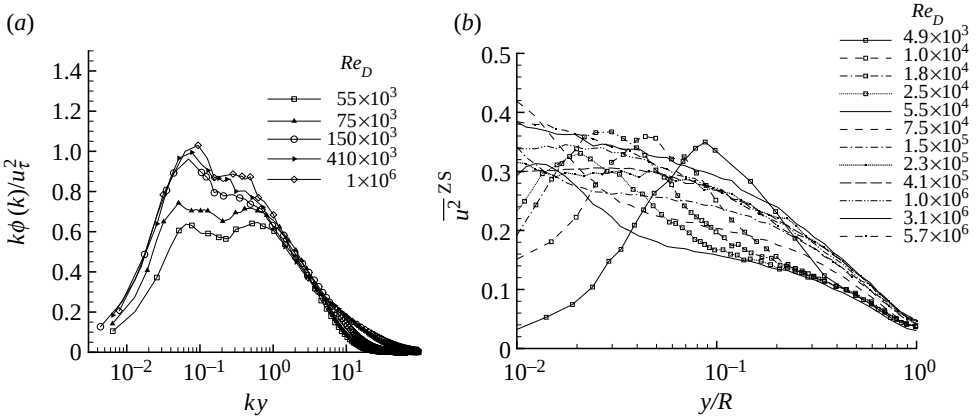

Figure 5. (*a*) Compensated spectra in inner scaling at constant wall-normal position $y/R=1$, various Reynolds numbers and (*b*) variation of $\overline{u^2}$ in ZS outer scaling (low Reynolds number data $4.9\times10^3 \leq Re_D \leq 25\times10^3$ from den Toonder & Nieuwstadt (1997)).

collapse reaches down to smaller values of y/R as the Reynolds number increases, before the profiles branch upwards to accommodate the near-wall fluctuation peak. While figure 5*a* demonstrates that there is spectral collapse with ky in an intermediate range of wavenumbers at $y/R=0.1$ for all Reynolds numbers, the effect of viscosity is apparent in $\overline{u^2}^+$ at the lower Reynolds numbers, appearing through reduced spectral energy in the wavenumber range corresponding to VLSMs and the lack of collapse at the high wavenumbers. These findings are also consistent with those of §2 concerning a lower limit for Reynolds similarity of the outer flow. It is unlikely that this interpretation of data in the outer region is affected by resolution at even the highest Reynolds number.

In order to assess self-similarity of subrange scales, we use the same data pre-multiplied in the form

$$f(k_1\eta) = \frac{(k_1\eta)^{5/3}\phi_{11}(k_1\eta)}{u_k^2}$$
$$f'(k_1S^*) = \frac{(k_1S^*)^{5/3}\phi_{11}(k_1S^*)}{u_\tau^2}. \tag{3.1}$$

Note that $S^* \approx \kappa y$ is in the log law region and $u_k=(\nu\epsilon)^{1/4}$ is the Kolmogorov velocity scale. In regions of simultaneous overlap, in the range $1/S^* \ll k_1 \ll 1/\eta$ where $f(k_1\eta)=f'(k_1S^*)=C$, $k_1^{-5/3}$ scaling of the spectrum is also expected. If $C=C_K$, the spectra are consistent with universal Kolmogorov scaling. The former represents development of the spectrum towards a Reynolds number independent form, while the latter may have stronger implications as an approach to local isotropy, as discussed further below.

We examine streamwise velocity spectra in the form of equations (3.1) at two Reynolds numbers, 75×10^3 and 1.0×10^6, corresponding to $R^+=1.5\times10^3$ and 19.7×10^3, respectively, for $0.05\leq y/R\leq0.12$. Figure 6*a–d* show the data in the ranges $90<y^+<220$ and $1000<y^+<2350$ for these Reynolds numbers. At both Reynolds numbers, $f'(k_1S^*)$ and $f(k_1\eta)$ appear to be approximately

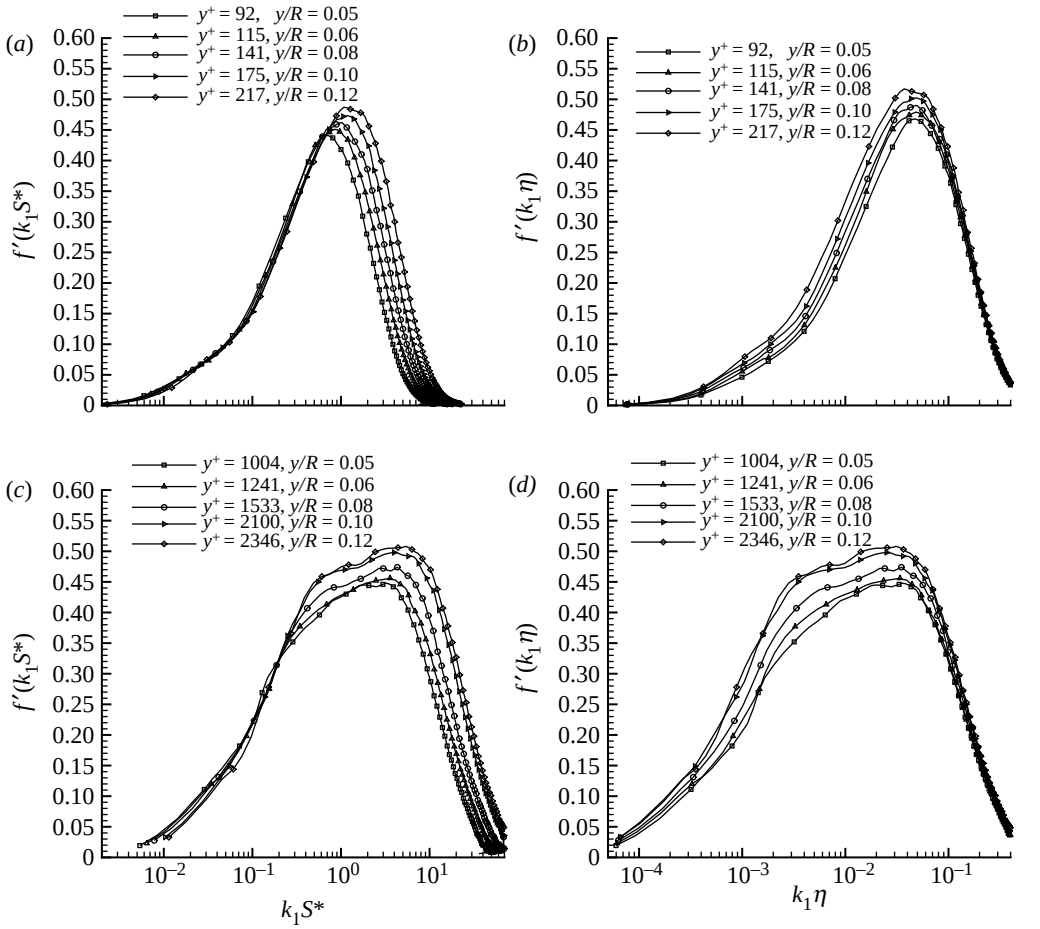

Figure 6. Pre-multiplied spectra in the overlap region using shear and Kolmogorov scaling, (*a*, *b*) $Re_D = 75\times10^3$ and (*c*, *d*) $Re_D = 1.0\times10^6$.

independent of y^+ for low k_1S^* and high $k_1\eta$. The former result is consistent with the inner scaling of figure 4*b* and indicates an upper limit of collapse of $kS^*\approx1$, while the collapse to a single $f(k_1\eta)$ in each case confirms that, for $k_1\eta<0.3$, spatial resolution does not affect these data. For intermediate wavenumbers, however, the spectra exhibit noticeably different forms which depend on wall-normal position.

For both Reynolds numbers, the ordinate increases with increasing y^+, but the profiles are much broader at the higher Reynolds number, with an apparent inflection point or 'shoulder', developing in the region of $k_1\eta=10^{-2}$: this becomes more noticeable at larger distances from the wall. This behaviour is similar to the double peak observed in results from the high Reynolds number boundary layer study of Saddoughi and Veeravalli (1994; henceforth 'SV'), uniformly sheared turbulence (Ferchichi & Tavoularis 2000) and the three-dimensional spectrum from high-Reynolds number homogeneous simulations of isotropic turbulence, such as those by Kaneda *et al.* (2003). The 'spectral bump' at $k_1\eta\approx0.05$ is believed to correspond to the 'bottleneck' phenomenon (SV; Falkovich

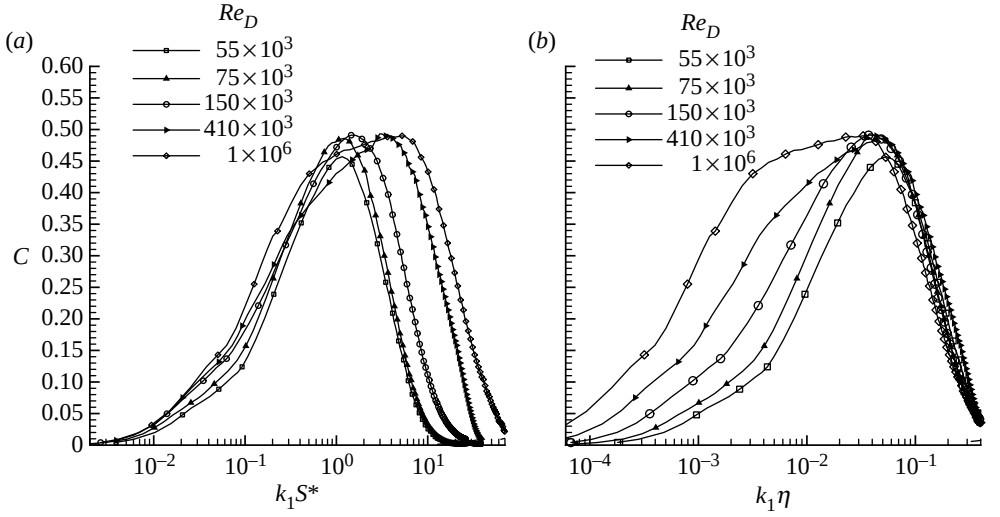

Figure 7. Pre-multiplied spectra at constant wall-normal location, $y/R=0.11$.

1994)—the energy transfer arising from the viscous suppression of triadic interactions caused by the rapid roll-off of the energy spectrum in the dissipation range. It is more pronounced in three-dimensional spectrum.

The data of SV, Mydlarski & Warhaft (1996), and Ferchichi & Tavoularis (2000) also confirm that the magnitude of $f(k_1\eta)$ increases, along with slight changes in the 5/3 scaling exponent, as $R_{\lambda T}$ increases. SV suggest that a $-5/3$ exponent is only reached when $R_{\lambda T}>1.5\times10^3$. The lack of collapse to a constant ordinate value for $k_1\eta<0.01$ indicates that the small-scale spectra in the overlap region do not demonstrate self-similarity and are therefore not described by purely inertial transfer. However, it can be speculated that this will be the limiting form for the small-scale spectrum for sufficiently high Reynolds number.

Figure 7*a*,*b* shows pre-multiplied spectra, $f(k\eta)$ and $f'(kS^*)$, at the outer edge of the overlap region, $y/R\approx0.1$, for increasing Reynolds numbers in the range $55\times10^3\leq Re_D\leq1.0\times10^6$. For these spectra, $95\leq R_{\lambda T}\leq600$ and $S^*/\eta=20$–180. The data at $Re_D=55\times10^3$ display a lower magnitude $C<C_K\approx0.5$ than observed at the other Reynolds numbers. At this Reynolds number, $R_{\lambda T}<100$ for all wall-normal locations traditionally associated with the overlap region in the mean velocity. For all higher Reynolds numbers, the data show a clear maximum at $k\eta\approx0.05$, and this peak value of $f(k\eta)$ and $g(kS^*)$ occurs at a slightly lower wavenumber than that for $Re_D=55\times10^3$. This result is in agreement with the findings of She *et al.* (1993) for isotropic turbulence at similar $R_{\lambda T}$. The data collapse well for higher wavenumbers and close to an expected value for the ordinate of approximately 0.5, indicating that the spectrum is fully developed at the small scales. Note that the peak in the vicinity of $k_1\eta=0.05$ occurs in the wavenumber range previously identified as that corresponding to the spectral bottleneck. For wavenumbers below the shoulder in the vicinity of $k_1\eta\approx0.01$, the data approach a constant value of C as the Reynolds number increases.

The present results can be compared to those of SV in terms of the ratio of k_1 to $1/S^*$. The shear-stress co-spectrum, $\phi_{12}(k_1)$, is the most sensitive indicator of local isotropy. Lumley (1967) has suggested that, by use of a local-wavenumber

definition of spectral flux, the shear-stress co-spectrum in the inertial region should scale as $k^{-7/3}S^{*-2/3}$. SV observed a lower limit of $kS^*=1$ for this scaling which corresponded to the lower limit of $k^{-5/3}$ scaling in the $\phi_{11}(k_1)$ spectrum.

The data of figure 7 demonstrate that C first reaches a constant value in the vicinity of $k\eta=0.05$ when $Re_D=75\times10^3$, and this corresponds to $kS^*\approx1$. This Reynolds number collapse to a constant value supports the lower limit of $kS^*\approx1$ for the appearance of a region of $k^{-5/3}$ scaling, which here is very short, but has been identified in other work as both the first-order inertial subrange and the emergence of the spectral bottleneck. This Reynolds number independent form of $f(k\eta)$ can thus be seen to occur when $S^*/\eta\approx1/0.05=20$, or since $S^*/\eta\sim y^{+3/4}$ in the overlap region, $y^+\approx150$. Note that the largest separation of S^* and η in the overlap region will also be observed at its outer limit; hence a minimum Reynolds number at which this can occur can then be found from the outer limit of the log law, $R^+=150/0.12=1.25\times10^3$. It is at this Reynolds number and wall-normal location that $R_{\lambda\mathrm{T}}$ first exceeds 100, in excellent agreement with arguments concerning the validity of the zeroth law. Note also the correspondence with the Reynolds number beyond which the value of ξ in figure 2*b* begins to rapidly decrease, and the associated changes in the mean velocity described above.

As the Reynolds number increases, figure 7 reveals an extension of collapse in Kolmogorov scaling to lower $k_1\eta$ values (improving the definition of the spectral bump) until a point of inflection, or shoulder, emerges at $k\eta\approx0.01$ (figure 6*d*). It is suggested that this represents a lower limit to the spectral bump, implying that its range of existence is defined in $k_1\eta$ (such that it is not self-similar). Although it is hard to determine the lower limit of this region in inner scaling, it does not appear to contradict the arguments above where $kS^*\approx1$. Thus, the spectral bump is completely defined if $S^*/\eta>1/0.01=100$ or $y^+\approx1100$, and at lower wavenumbers a region of approximately constant, lower C emerges (in agreement with the SV data). This region of approximate $k^{-5/3}$ scaling of the spectrum will only appear at $y/R=0.12$ for $R^+\geq9\times10^3$ ($Re_D\geq500\times10^3$).

SV proposed that for $kS^*\geq3$, all three velocity components demonstrate $k^{-5/3}$ scaling and obey isotropic relationships to each other. $kS^*\geq10$ corresponded to a stronger indication of local isotropy than the lower limits through an approximately zero shear-stress correlation coefficient spectrum. There is insufficient high Reynolds number data to examine the structure of the flow under the stricter conditions for local isotropy suggested by SV: when $kS^*=3$ and $kS^*=10$ at $k\eta=0.01$ the corresponding Kármán numbers are $40\times10^3<R^+<210\times10^3$. One can speculate that these conditions correspond to increasingly better approximations to local isotropy (in terms of all three velocity components), K41 scaling and an approximately constant value of $C=C_{\mathrm{K}}$.

4. A picture of high Reynolds number wall-bounded flows

The results of the preceding sections have demonstrated that significant development of turbulent pipe flow occurs as the Reynolds number is increased until at least $Re_D<230\times10^3$ or $R^+=5\times10^3$, and this is observed in measurements of the mean and second moment of the fluctuating streamwise velocity, and the associated friction factor data and velocity spectra. Moreover, it has been shown that conditions for the zeroth law of turbulence to hold are not

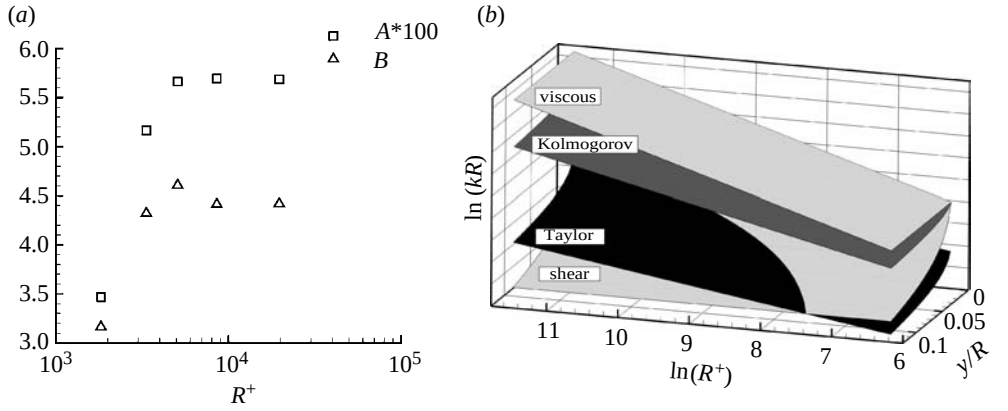

Figure 8. (*a*) Non-dimensional dissipation rate estimates, $y/R=0.12$: $A=(u_\tau/u_\mathrm{K})^3/(R/\eta)$, $B=((U_\mathrm{cl}-\bar{U})/u_\mathrm{K})^3/(R/\eta)$; (*b*) schematic of the variation of scale variation with distance from the wall and Reynolds number, after Dimotakis (2000).

met in the expected overlap region at all Reynolds numbers and this is reflected in the development of the streamwise spectrum in the range that exhibits approximate $-5/3$ scaling which, in agreement with the results of many other workers, clearly does not necessarily imply local isotropy. Here, we attempt to provide a consistent interpretation of the data in real and wavenumber space for the Reynolds number range $55\times10^3\leq Re_D\leq1.0\times10^6$, at the upper end of which the turbulence exhibits features that may be described as 'fully developed'.

The zeroth law of turbulence indicates that the non-dimensional dissipation rate tends to a constant with increasing Reynolds number. In the local-equilibrium region, scales are simply related so that appearance of the zeroth law appears as spectral collapse in figure 7, i.e. the appearance of a first-order inertial subrange. It follows that there is a required minimum spectral separation of energy and dissipation scales and, using a locally isotropic approximation for the dissipation, it can be shown that $R_{\lambda\mathrm{T}}\sim(\lambda_\mathrm{T}/\eta)^2$. By implication, local equilibrium and, more precisely, inertial scaling cannot be expected in either a spectral or spatial sense below the scale separation implied by the zeroth law, where it can be inferred that spatial transport is always non-negligible. Local equilibrium as an approximation to the spectral transfer thus represents a link between similarity in physical and spectral space in the overlap region, where the additional complexity of a net spatial energy flux is reduced as the Reynolds number becomes sufficiently high for both physical and spectral scale separation. A further demonstration of this scale separation (and one that comes from estimation of scales which are free of any resolution effects) can be provided by estimating the dissipation rate as

$$\epsilon=\frac{u_\mathrm{K}^3}{\eta}=\frac{u_\tau^3}{AR}=\frac{(U_\mathrm{cl}-\bar{U})^3}{BR}, \tag{4.1}$$

where A and B are constants. As shown in figure 8*a*, the non-dimensional forms of the dissipation rate become independent of Reynolds numbers only for $R^+>5000$. Here, estimates for ϵ are made by invoking the local-equilibrium approximation.

Unidirectional mean shear in wall-bounded flows leads to the anisotropic production of turbulence energy. In this case, the spectrum at wavenumbers $k = O(1/S^*)$ is dominated by shear production and (anisotropic) inter-component energy transfer. In addition, the blocking effect of the wall maintains anisotropy in scales larger than $O(y)$, such that only scales significantly smaller than y, where, in the logarithmic region, $S^* \sim y$ (assuming local equilibrium), can ever approach local isotropy.

For self-similarity of the spectrum at scales in the inertial range not only λ_T/η must be sufficiently high, but also there must be a suitable separation of the shear and dissipation scales, i.e. $S^*/\eta \gg 1$ (while local isotropy is required for spectral universality). Note that λ_T is a mixed scale and hence is not itself a suitable candidate for testing the appearance of universal scaling. Here, the effect of the boundary conditions is considered through S^*. Interestingly, S^* equally well describes the effect of the no-slip condition as well as that of blocking (the impermeability constraint), because in the overlap region $\partial U/\partial y \sim 1/y$.

Non-zero spatial transport constitutes a source or a sink at each wavenumber such that local isotropy is not possible since the spectral energy flux is not conservative. However, relaxation of the requirement of local isotropy but requiring that sources and sinks are small in comparison with spectral flux corresponds to both the 'nearly inertial' turbulence (Lumley 1964) and the 'first-order inertial subrange' of Bradshaw. In terms of self-similarity, the small-scale streamwise spectrum in the overlap region approaches an asymptotic, fully developed form, only if $S^*/\eta > 100$. Further increases in local Reynolds number (y^+) at a given wall-normal location broaden the subrange region. Note that this does not preclude changes with Reynolds numbers at much larger scales $kS^* \ll 1$. At the lower Reynolds numbers, the spectra exhibit the direct effects of viscosity at large as well as small scales, as demonstrated by the deterioration in collapse at both ends of the spectrum. This is also apparent in the scaling of $\overline{u'^2}^{ZS}$ in figure 5*b*. However, if the condition that $S^*/\eta > 100$ is not met, the Reynolds number is too low for inertially dominated turbulence, as proposed by Wosnik *et al.* (2000). Those authors suggested a lower limit of $R^+ \approx 3000$, which has been refined here due to the combination of mean velocity and streamwise spectral information from the Superpipe.

Figure 8*b* shows a schematic of the development of scale separation with Reynolds number in the overlap region and is an extension to the two-dimensional plots of Dimotakis (2000), which showed the separation of scales required for spatial and spectral self-similarity in a wide range of flows, and Tennekes & Lumley (1972). The separations of shear, Taylor and Kolmogorov scales within the overlap region increase with Reynolds number and it has been argued here that a necessary, but not sufficient, condition for self-similar $k^{-5/3}$ scaling of the streamwise spectrum (and by implication also inertial scaling in the K41 sense) is given by

$$\nu/u_\tau < \eta < \lambda_T < S^* < R. \tag{4.2}$$

Outside the overlap region, the local-equilibrium approximation does not apply and S^*, λ_T and η are not simply related. However, the peak value of $R_{\lambda T}$ occurs within the outer region. Thus, self-similar scaling is likely to begin in the core and spread to the centreline and overlap region as the Reynolds number increases. At low local Reynolds numbers, $R_{\lambda T} < 100$, the validity of the dissipation approximation deteriorates, but it appears that $\lambda_T > S^*$, precluding self-similarity of $\overline{u^2}$.

Wosnik *et al.* (2000) described the importance of a 'mesolayer' in which the influence of viscosity remained due to insufficient scale separation for inertially dominated turbulence in internal flows, a conclusion which present work strongly supports. As George & Castillo (1997) indicated, the same idea of scale separation for inertial scaling can be applied to the zero-pressure-gradient turbulent boundary layer, revealing similar behaviour to that documented above for pipe flow. Note, however, that those authors propose a power law for the boundary layer mean velocity. In the classical log layer model, the wake factor describing the deviation of the outer flow from a log law has a similar form to that of ξ in the pipe (but with the extrapolated value of the log law at the edge of the boundary layer, δ, instead of the average velocity) such that $\Delta U/u_\tau = (U_\infty - U_{\log,y=\delta})/u_\tau$. The classical work of Coles (1962) shows that the wake factor increases with Reynolds number to a maximum in the region of $Re_\theta = 6000$ ($Re_{\delta^*} \approx 0.9 \times 10^4$) then decreases until $Re_\theta \approx 15\,000$ ($Re_{\delta^*} \approx 2.3 \times 10^4$), beyond which it appears to attain a constant value of slightly larger than 2. Based on the former Re_{δ^*}, the comparable pipe Reynolds number is $Re_D = 400 \times 10^3$, in apparent agreement with the suggestion that there is similar Reynolds number behaviour in both flows.

Dimotakis (2000) identified the decoupling of viscous and large-scale effects implied by the zeroth law in shear flows with a wide range of imposed anisotropy, calling it the 'mixing transition'. He proposed that it is a universal condition in turbulent flows and a criterion for 'fully developed turbulence' (the sustenance of three-dimensional turbulent fluctuations) occurring in the vicinity of $R_{\lambda T} = 100$ or a Reynolds number based on displacement thickness, $Re_{\delta^*} \approx 10^4$. Beyond this scale decoupling, enhanced mixing and independence of the large scales from viscosity were demonstrated for a range of flows. Interestingly, the Reynolds number at which self-similarity appears in the present data coincides approximately with that suggested by Wygnanski & Champagne (1973) for the end of the 'slug' regime in pipe flow.

5. Conclusions

Streamwise velocity data from the Princeton Superpipe have been used to show how the inertial overlap region may be described as a spatial analogue of the inertial subrange, and be used to explain the gradual approach to asymptotic, high Reynolds number pipe flow. When the local Reynolds number in the region $\nu/u_\tau \ll y \ll R$ is too low for the zeroth law to hold, the local-equilibrium approximation is not a good one and there is an insufficient separation of production and dissipation scales for inertially dominated turbulence to exist, so that self-similarity of the small scales is not possible, as recently indicated by the work of George and co-authors. The power of the local-equilibrium approximation as an indicator of inertially dominated turbulence in both physical and spectral space is not a new concept, but one that is often neglected in the discussions of asymptotic behaviour in turbulent pipe flow.

The authors would like to thank Lex Smits for continuing use of the Superpipe data and insightful discussions, Jiang Wei-Min for experimental measurements and Paul Dimotakis for suggesting figure 8*b*. B.J.M. held a Royal Society Dorothy Hodgkin Fellowship for the duration of the majority of this work and J.F.M. was funded through the Leverhulme Trust (grant F/07058/H). The support of these sponsors is gratefully acknowledged.

References

Bradshaw, P. 1967 Conditions for the existence of an inertial subrange in turbulent flow. Natl Phys. Lab. Aero. Rep. No. 1220.

Coles, D. E. 1962 The turbulent boundary layer in a compressible fluid. Appendix A: a manual of experimental boundary-layer practice for low-speed flow. Rand. Corp. Rep. R-403-PR, ARC 24473.

den Toonder, J. M. J. & Nieuwstadt, F. T. M. 1997 Reynolds number effects in a turbulent pipe flow for low to moderate *Re*. *Phys. Fluids* **9**, 3398–3409. (doi:10.1063/1.869451)

Dimotakis, P. E. 2000 The mixing transition in turbulent flows. *J. Fluid Mech.* **409**, 69–98. (doi:10.1017/S0022112099007946)

Durbin, P. A. & Speziale, C. G. 1991 Local anisotropy in strained turbulence at high Reynolds numbers. *J. Fluids Eng.* **113**, 707–709.

Falkovich, G. 1994 Bottleneck phenomenon in developed turbulence. *Phys. Fluids* **6**, 1411–1414. (doi:10.1063/1.868255)

Ferchichi, M. & Tavoularis, S. 2000 Reynolds number effects on the fine structure of uniformly sheared turbulence. *Phys. Fluids* **12**, 2942–2953. (doi:10.1063/1.1311610)

Frisch, U. 1995 *Turbulence. The legacy of A. N. Kolmogorov*. Cambridge, UK: Cambridge University Press.

George, W. K. & Castillo, L. 1997 Zero-pressure-gradient boundary layer. *Appl. Mech. Rev.* **59**, 689–729.

Kaneda, Y., Ishihara, T., Tokokawa, M., Itakura, K. & Uno, A. 2003 Energy dissipation rate and energy spectrum in high resolution direct numerical simulations of turbulence in a periodic box. *Phys. Fluids* **15**, L21–L24. (doi:10.1063/1.1539855)

Kim, K. C. & Adrian, R. J. 1999 Very large-scale motion in the outer layer. *Phys. Fluids* **11**, 417–422. (doi:10.1063/1.869889)

Kolmogorov, A. N. 1941 The local structure of turbulence in incompressible viscous fluid for very large Reynolds numbers. *Dokl. Akad. Nauk SSSR* **30**, 301–305.

Kolmogorov, A. N. 1962 A refinement of previous hypotheses concerning the local structure of turbulence in a viscous incompressible fluid at high Reynolds numbers. *J. Fluid Mech.* **13**, 82–85. (doi:10.1017/S0022112062000518)

Lawn, C. J. 1971 The determination of the rate of dissipation in turbulent pipe flow. *J. Fluid Mech.* **48**, 477–505. (doi:10.1017/S002211207100171X)

Long, R. L. & Chen, T.-C. 1981 Experimental evidence for the existence of the 'mesolayer' in turbulent systems. *J. Fluid Mech.* **105**, 19–59. (doi:10.1017/S0022112081003108)

Lumley, J. L. 1964 The spectrum of nearly inertial turbulence in a stably stratified fluid. *J. Atmos. Sci.* **21**, 99–102. (doi:10.1175/1520-0469(1964)021<0099:TSONIT>2.0.CO;2)

Lumley, J. L. 1967 Similarity and the turbulent energy spectrum. *Phys. Fluids* **10**, 855–858. (doi:10.1063/1.1762200)

Marati, N., Casciola, C. M. & Piva, R. 2004 Energy cascade and spatial fluxes in wall turbulence. *J. Fluid Mech.* **521**, 191–215. (doi:10.1017/S0022112004001818)

McKeon, B. J., Li, J., Jiang, W., Morrison, J. F. & Smits, A. J. 2004 Further observations on the mean velocity distribution in fully-developed turbulent pipe flow. *J. Fluid Mech.* **501**, 135–147. (doi:10.1017/S0022112003007304)

McKeon, B. J., Zagarola, M. V. & Smits, A. J. 2005 A new friction factor relationship for fully developed pipe flow. *J. Fluid Mech.* **538**, 429–443. (doi:10.1017/S0022112005005501)

Mestayer, P. 1982 Local isotropy and anisotropy in a high-Reynolds-number turbulent boundary layer. *J. Fluid Mech.* **125**, 475–503. (doi:10.1017/S0022112082003450)

Millikan, C. M. 1938 A critical discussion of turbulent flows in channels and circular tubes. In *Proc. 5th Int. Congr. Appl. Mech.* New York, NY: Wiley.

Morrison, J. F., Jiang, W., McKeon, B. J. & Smits, A. J. 2004 Scaling of the streamwise velocity component in turbulent pipe flow. *J. Fluid Mech.* **508**, 99–131. (doi:10.1017/S0022112004008985)

Mydlarski, L. & Warhaft, Z. 1996 On the onset of high-Reynolds-number grid-generated wind tunnel turbulence. *J. Fluid Mech.* **320**, 331–368. (doi:10.1017/S0022112096007562)

Nickels, T. B., Marusic, I., Hafez, S. & Chong, M. S. 2005 Evidence of the k^{-1} law in a high Reynolds number boundary layer. *Phys. Rev. Lett.* **95**, 074501. (doi:10.1103/PhysRevLett.95.074501)

Nikuradse, J. 1932 Laws of turbulent flow in smooth pipes (English translation). NASA TT F-10 (1966).

Saddoughi, S. G. & Veeravalli, S. V. 1994 Local isotropy in turbulent boundary layers at high Reynolds number. *J. Fluid Mech.* **268**, 333–372. (doi:10.1017/S0022112094001370)

She, Z.-S., Chen, S., Doolen, G., Kraichnan, R. H. & Orszag, S. O. 1993 Reynolds number dependence of isotropic Navier–Stokes turbulence. *Phys. Rev. Lett.* **70**, 3251–3254. (doi:10.1103/PhysRevLett.70.3251)

Sreenivasan, K. R. 1998 An update on the energy dissipation rate in isotropic turbulence. *Phys. Fluids* **10**, 528–529. (doi:10.1063/1.869575)

Taylor, G. I. 1935 Statistical theory of turbulence. *Proc. R. Soc. A* **151**, 421–444.

Tennekes, H. & Lumley, J. L. 1972 *A first course in turbulence*. Cambridge, MA: MIT Press.

Wosnik, M., Castillo, L. & George, W. K. 2000 A theory for turbulent pipe and channel flows. *J. Fluid Mech.* **421**, 115–145. (doi:10.1017/S0022112000001385)

Wygnanski, I. J. & Champagne, F. H. 1973 On transition in a pipe. Part 1. The origin of puffs and slugs and the flow in a turbulent slug. *J. Fluid Mech.* **59**, 281–335. (doi:10.1017/S0022112073001576)

Yaglom, A. M. 1979 Similarity laws for constant-pressure and pressure-gradient turbulent wall flows. *Annu. Rev. Fluid Mech.* **11**, 505–540. (doi:10.1146/annurev.fl.11.010179.002445)

Zagarola, M. V. 1996 Mean-flow scaling of turbulent pipe flow. Ph.D. thesis, Princeton University, Princeton, NJ.

Zagarola, M. V. & Smits, A. J. 1998 Mean flow scaling in turbulent pipe flow. *J. Fluid Mech.* **373**, 33–79. (doi:10.1017/S0022112098002419)